

# FedBoosting: Federated Learning with Gradient Protected Boosting for Text Recognition

Hanchi Ren, Jingjing Deng\*, Xianghua Xie\*, Xiaoke Ma, Yichuan Wang

## Abstract

Conventional machine learning methodologies require the centralization of data for model training, which may be infeasible in situations where data sharing limitations are imposed due to concerns such as privacy and gradient protection. The Federated Learning (FL) framework enables the collaborative learning of a shared model without necessitating the centralization or sharing of data among the data proprietors. Nonetheless, in this paper, we demonstrate that the generalization capability of the joint model is suboptimal for Non-Independent and Non-Identically Distributed (Non-IID) data, particularly when employing the Federated Averaging (FedAvg) strategy as a result of the weight divergence phenomenon. Consequently, we present a novel boosting algorithm for FL to address both the generalization and gradient leakage challenges, as well as to facilitate accelerated convergence in gradient-based optimization. Furthermore, we introduce a secure gradient sharing protocol that incorporates Homomorphic Encryption (HE) and Differential Privacy (DP) to safeguard against gradient leakage attacks. Our empirical evaluation demonstrates that the proposed Federated Boosting (FedBoosting) technique yields significant enhancements in both prediction accuracy and computational efficiency in the visual text recognition task on publicly available benchmarks.

## 1 Introduction

The protection of personal data and preservation of privacy have garnered considerable interest from researchers in recent years [1, 2, 3, 4, 5, 6, 7]. Traditional machine learning methodologies necessitating centralized data for model training may be infeasible due to data sharing restrictions. Consequently, decentralized data-training approaches are increasingly appealing, as they offer advantages in preserving privacy and ensuring data security. Federated Learning (FL) [8, 9] was introduced to address these concerns by enabling individual data providers to collaboratively train a shared global model without the need for central data aggregation. McMahan *et al.*

[9] proposed a practical decentralized training method for deep networks based on averaging aggregation. Empirical studies conducted on various datasets and architectures demonstrated the robustness of FL for handling unbalanced and Independent and Identically Distributed (IID) data. While frequent updating generally leads to improved prediction performance, communication costs can increase substantially, particularly for large datasets [10, 11, 9, 12, 13]. To address the efficiency issue, Konečný *et al.* [11] proposed two weight updating methods based on Federated Averaging (FedAvg), namely structured updates and sketched updates approaches, to reduce the up-link communication costs associated with transmitting gradients from local machines to a centralized server.

Prediction performance and data privacy represent two primary challenges in FL research. On the one hand, the accuracy of FL is known to decline considerably when applied to Non-Independent and Non-Identically Distributed (Non-IID) data [14, 15, 16, 17, 18, 19, 20, 21, 22]. Zhao *et al.* [14] demonstrated that weight divergence can be quantitatively measured using Earth Mover’s Distance (EMD) between class distributions on each local machine and the global population distribution. Consequently, they proposed sharing a small subset of data among all edge devices to enhance model generalization on Non-IID data. However, this strategy may not be viable when data sharing restrictions are in place, potentially leading to privacy breaches. Li *et al.* [23] examined the convergence properties of FedAvg and identified a trade-off between its communication efficiency and convergence rate, arguing that the model converges slowly on heterogeneous datasets. Our empirical study in this paper confirms that, given Non-IID datasets, the training process requires considerably more iterations to reach an optimal solution and often fails to converge, particularly when local models are trained on large-scale datasets with a small batch size, or the global model is aggregated after a substantial number of epochs. The feasibility of adaptive aggregation by leveraging training and testing outcomes has been established [24, 25]. On the other hand, model gradients are generally considered safe to share in FL systems for model aggregation. Nonetheless, some studies have revealed the feasibility of recovering training data information from model gradients. For instance, Fredrikson *et al.* [26] and Melis *et al.* [27] reported two methods capable of identifying a sample with specific properties in the training batch.

\*First Author: H. Ren (hanchi.ren@swansea.ac.uk). Corresponding Authors: J. Deng (jingjing.deng@durham.ac.uk) and X. Xie (x.xie@swansea.ac.uk). Co-Authors: X. Ma (xkma@xidian.edu.cn) and Y. Wang (chuan@xaut.edu.cn).

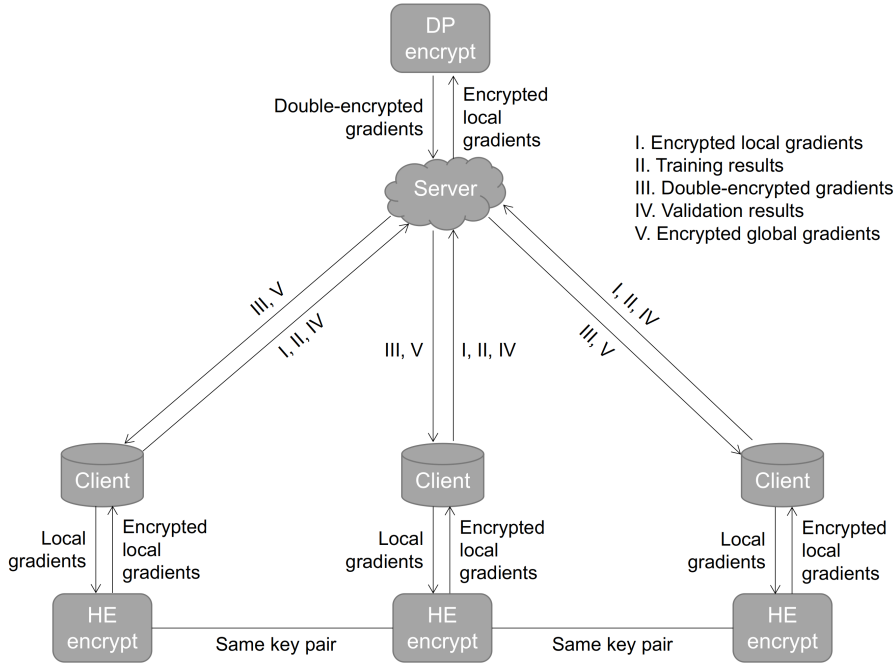


Figure 1: The schematic diagram illustrates the proposed FedBoosting and encryption protocol. For demonstration purposes, two clients are depicted; however, the proposed method is designed to accommodate an arbitrary number of local clients.

Hitaj *et al.* [28] proposed a Generative Adversarial Network (GAN) model as an adversarial client for estimating data distribution from the outputs of other clients without access to their training data. Zhu *et al.* [29] and Zhao *et al.* [30] demonstrated that data recovery can be framed as a gradient regression problem, assuming the gradient from a targeted client is available, which is a largely valid assumption in most FL systems. Moreover, the Generative Regression Neural Network (GRNN) proposed by Ren *et al.* [31] comprises two branches of generative models: one based on GAN for generating fake training data and the other on a fully-connected layer for generating corresponding labels. The training data is revealed by regressing the true gradient and the fake gradient generated by the fake data and relevant label.

In this paper, we propose FedBoosting method to address the weight divergence and gradient leakage issues in general FL framework. Instead of treating individual local models equally when the global model is aggregated, we consider the data diversity of local clients in terms of the status of convergence and the ability of generalization. To address the potential risk of data leakage via shared gradients, a Differential Privacy (DP) based linear aggregation method is proposed using Homomorphic Encryption (HE) [32] to encrypt the gradients which provides two layers of protection. The proposed encryption scheme only leads to a negligible increase in computational cost.

In this paper, we introduce the FedBoosting method to address weight divergence and gradient leakage issues within the general FL framework. Rather than treating

individual local models equally during global model aggregation, we take into account the data diversity of local clients concerning their convergence status and generalization ability. To mitigate the potential risk of data leakage via shared gradients, we propose a DP-based linear aggregation method using HE [32] to encrypt gradients, providing dual layers of protection. The proposed encryption scheme incurs only a negligible increase in computational cost.

We evaluate the proposed method on text recognition task using public benchmarks, as well as a binary classification task on two datasets, demonstrating its superiority in terms of convergence speed, prediction accuracy, and security. We also assess the performance reduction due to encryption. Our contributions can be summarized in four main points:

- We propose a novel aggregation strategy, FedBoosting, for FL to address weight divergence and gradient leakage issues. Empirically, we demonstrate that FedBoosting converges considerably faster than FedAvg, while maintaining communication costs comparable to traditional approaches. Particularly when local models are trained with small batch sizes and the global model is aggregated after a large number of epochs, our approach can still converge to a reasonable optimum, whereas FedAvg often fails in such cases.
- We introduce a dual-layer protection scheme utilizing HE and DP to encrypt gradients exchanged between

servers and clients, safeguarding data privacy against gradient leakage attacks.

- We demonstrate the feasibility of our method on two datasets by visually evaluating decision boundaries. Additionally, we showcase its superior performance in a visual text recognition task on multiple large-scale Non-IID datasets compared to centralized approaches and FedAvg. The experimental results confirm that our approach outperforms FedAvg in terms of convergence speed and prediction accuracy, suggesting that the FedBoosting strategy can be integrated with other Deep Learning (DL) models in privacy-preserving scenarios.
- We provide a publicly available implementation of the proposed FedBoosting method to ensure reproducibility. The implementation can also be executed in a distributed, multi-Graphics Processing Units (GPUs) setup.<sup>1</sup>

The remainder of this paper is organized as follows: In Section 2, we present related work on encryption methods, collaborative learning, and gradient leakage. The proposed FedBoosting method and corresponding encryption techniques are described in Section 3 and evaluated using a text recognition task and a binary classification task. Section 4 provides details of the experiments, discussions on the results, and a performance comparison. Finally, we draw conclusions in Section 5.

## 2 Related Work

FL has been proposed for privacy-preserving machine learning to train models across multiple decentralized edge devices or clients containing local data samples [9, 11, 8, 33, 34, 35]. The FL framework retains raw data with the owners and trains models locally at individual client nodes, while gradients from these models are exchanged and aggregated rather than the data. Compared to Secure Multi-Party Computation (MPC) [36, 37], which provides high security at the cost of expensive cryptographic operations, FL allows for more efficient implementation and reduced running costs due to its relaxed security requirements. As explicit data exchange is not required, FL does not necessitate the addition of noise to the data as in DP [38, 39, 40, 41, 42], nor the encryption of data into a homomorphic phase for homomorphic operations as in HE [43, 1, 44, 45]. Gradient aggregation from local models constitutes a core research problem in FL. McMahan *et al.* [9] presented the FedAvg method for training deep neural networks across multiple parties, whereby the global model averages gradients from local models, *i.e.*  $\omega' = \sum_i^N \frac{1}{N} \omega_i$ , with  $\omega'$  and  $\omega_i$  representing the gradients of

the global and  $i_{th}$  local models, respectively, and  $N$  denoting the total number of clients. The method was evaluated on the MNIST benchmark, demonstrating its feasibility for classic image classification tasks using Convolutional Neural Network (CNN) as the learning model. Although the experimental results indicate that FedAvg is suitable for both IID and Non-IID data, the statistical challenge of FL remains when local models are trained on large-scale Non-IID data. Our experimental results support this assertion, as the prediction accuracy and convergence rate significantly decline with large-scale Non-IID data when using FedAvg.

FL is designed for privacy-preserving training, as data is retained and processed locally. Nevertheless, multiple studies, such as [28, 29, 31], have underscored that FL is susceptible to the gradient leakage problem, whereby private training data can be recovered from publicly shared gradients with a considerably high success rate. Hitaj *et al.* [28] proposed a training data recovery approach for FL systems using GANs. This approach aims to generate training samples similar to a specific class, rather than directly recovering the original training data. Initially, the global FL model is trained for several iterations to achieve relatively high accuracy. The authors assume that a malicious participant can obtain a client model, which is then used as a discriminator. Subsequently, an image generator is updated based on the output of the discriminator for a targeted image class. Ultimately, the well-trained generator can produce image samples resembling the training data for the specified image class. Zhu *et al.* [29] framed the data recovery task as a gradient regression problem, treating pixel values of the input image as random variables optimized using back-propagation while the shared model parameters remain fixed. The objective function measures the Euclidean distance between the shared gradient in FL and the gradient generated by the random image input, which is minimized during the training phase. They posited that the optimized input would closely resemble the original training image stored on the local client. Experimental results on public benchmark datasets substantiate this hypothesis, thereby indicating that gradient sharing could potentially result in privacy data leakage. Our prior work, GRNN [31], further enhances the success rate of leakage attacks using generative models for data recovery, particularly when employing a large batch size in training.

## 3 Proposed Method

### 3.1 FedBoosting Framework

The FedAvg method [9] generates a new model by averaging gradients from local clients. Nonetheless, with Non-IID data, the weights of local models may converge in divergent directions due to disparities in data distribution. As a result, simple averaging schemes perform inadequately, particularly in the presence of strong bias and extreme

<sup>1</sup><https://github.com/Rand2AI/FedBoosting>

outliers [14, 23, 46]. Consequently, we propose the use of a boosting scheme, specifically FedBoosting, to adaptively combine local models based on their generalization performance on distinct local validation datasets. Simultaneously, to preserve data privacy, information exchange among decentralized clients and the server is restricted. Instead of sharing data between clients, encrypted local models are exchanged through a centralized server and validated independently on each client. Further details can be found in Figure 1.

---

**Algorithm 1** FedBoosting with HE and DP: Server

---

```

1: build model and initialize weights  $\omega_0$ ;
2: for each round  $r = 1, 2, \dots, R$  do
3:   for each client  $i \in C_N$  do
4:     if  $r == 1$  then
5:        $g_r^{*i}, T_r^i \leftarrow \text{Train}(r, i, \omega_{r-1})$  via Algorithm 2.a;
6:     else
7:        $g_r^{*i}, T_r^i \leftarrow \text{Train}(r, i, G_{r-1}^{*i})$  via Algorithm 2.a;
8:     end if
9:   end for
10:  for each client  $i \in C_N$  do
11:    generate  $\hat{G}_r^{*i}$  via Equ. (5);
12:     $V_r^i \leftarrow \sum_j^N \text{Evaluate}(j, \hat{G}_r^{*i})$  via Algorithm 2.b;
13:  end for
14:  generate  $p_r^i$  via Equ. (2&3);
15:  generate  $G_r^*$  via Equ. (4);
16:  if  $r == R$  then
17:     $\omega_r \leftarrow \text{Decrypt}(G_r^*)$  via Algorithm 2.c
18:  end if
19: end for

```

---

In contrast to FedAvg, the proposed FedBoosting method accounts for the fitness and generalization performance of each client model, adaptively merging the global model using varying weights for all client models. To accomplish this, three different pieces of information are generated from each client: local gradients  $G_r^i$ , training loss  $T_r^i$ , and validation loss  $V_r^{i,i}$ . Here,  $G_r^i$  and  $T_r^i$  represent the local gradients and training loss from the  $i$ -th local model in training round  $r$ , while  $V_r^{i,i}$  refers to the validation loss from the  $i$ -th local model on the  $i$ -th local validation dataset in training round  $r$ . The local gradients  $G_r^i$  are subsequently distributed to all other clients via a centralized server. Each client can then obtain cross-validated loss  $V_r^{i,j}$ , where  $i \neq j$ . Training and validation losses serve as two metrics for evaluating the predictive performance of the models. A model with a relatively large training loss typically indicates poor convergence and weak generalization capabilities. However, it also implies that the model gradient contains ample information for training. Conversely, a model with low training loss does not necessarily ensure good generalization ability (e.g., over-fitting) and may contain less training information. Therefore, we also consider validation loss. These two losses jointly determine the aggregation weight of a local model contributing to the global model, as depicted in Equation (2). Then, on the server, all validation results of the  $i$ -th model are summed, denoted as  $V_r^i$ , representing the  $i$ -th model's gen-

---

**Algorithm 2** FedBoosting with HE and DP: Client

---

**a. Train**( $r, i, \omega_{r-1} || G_{r-1}^{*i}$ ):

```

1: if  $i == 1$  then
2:   generate key pair and sent to other clients
3: else
4:   wait for key pair from  $C_1$ 
5: end if
6: if  $r == 1$  then
7:   load  $\text{Trn}D^i, \text{Val}D^i$ 
8: else
9:   decrypt  $G_{r-1}^{*i}$  to  $G_{r-1}$  by secret keys
10:   $\omega_{r-1} = \omega_{r-2} + G_{r-1}$ 
11: end if
12: for each epoch  $e = 1, 2, \dots, E$  do
13:   for each batch  $b = 1, 2, \dots, B$  do
14:      $\omega_r \leftarrow \omega_{r-1} - \eta \cdot \nabla f(\text{Trn}D^{i,b}, \omega_{r-1})$ 
15:   end for
16: end for
17:  $G_r^i = \omega_r - \omega_{r-1}$ 
18:  $g_r^i = \lfloor (G_r^i * 1e32) / P \rfloor$  and generate  $g_r^{*i}$  by public keys
19:  $T_r^i \leftarrow f(\text{Trn}D^i | \omega_r)$ 
20: return  $g_r^{*i}, T_r^i$  to server

```

**b. Evaluate**( $j, \hat{G}_r^{*i}$ ):

```

1: decrypt  $\hat{G}_r^{*i}$  to  $\hat{G}_r^i$  by secret keys
2:  $\hat{\omega}_r^i = \omega_{r-1} + \hat{G}_r^i$ 
3:  $V_r^{i,j} \leftarrow f(\text{Val}D^j | \hat{\omega}_r^i)$ 
4: return  $V_r^{i,j}$  to server

```

**c. Decrypt**( $G_r^*$ ):

```

1: decrypt  $G_r^*$  to  $G_r$  by secret keys
2:  $\omega_r = \omega_{r-1} + G_r$ 
3: return  $\omega_r$  to server

```

---

eralization capacity. Taking convergence into account, a *Softmax* layer is employed with input  $T_r$ . The outputs, combined with  $V_r^i$ , are utilized for calculating the aggregation weight  $p_r^i$ . In the current round of aggregation, the new global gradients  $G_r$  can be computed by merging all local gradients  $G_r^i$  in accordance with their respective weights  $p_r^i$ :

$$G_r = \sum_i^N p_r^i G_r^i, \forall p_r^i \in [0, 1], \quad (1)$$

$$p_r = \text{softmax}(\text{softmax}(T_r) \cdot \sum_j^N V_r^j), \quad (2)$$

$$V_r^{i,j} = \begin{pmatrix} V_r^{1,1} & V_r^{1,2} & \dots & V_r^{1,j} \\ V_r^{2,1} & V_r^{2,2} & \dots & V_r^{2,j} \\ \vdots & \vdots & \ddots & \vdots \\ V_r^{i,1} & V_r^{i,2} & \dots & V_r^{i,j} \end{pmatrix} \quad (3)$$

where  $T_r^i$  and  $p_r^i$  are training loss and mixture coefficient for the  $i$ -th local model. Moreover, the proposed FedBoosting approach is resistant to certain malicious attacks, such as data poisoning. For example, if a malicious client introduces poisoned data into the training set and the tainted local model is aggregated with the same weight as other uncontaminated models, our method can mitigate this issue as the validation scores of the compromised

model on other clients will be significantly lower, consequently resulting in a substantially reduced aggregation weight.

### 3.2 HE Aggregation with Quantized Gradient

HE ensures that computations can be performed on encrypted data as  $Enc(A) \bullet Enc(B) = Enc(A * B)$ , where “ $\bullet$ ” represents operations on encrypted data, and “ $*$ ” represents operations on plaintext data. Since FedBoosting involves computing the global model based on local gradients, HE is utilized in our method to guarantee secure aggregation and gradient exchange among clients and the server. In FedBoosting, local models are trained on each client, and subsequently, local gradients are transmitted to the server, where all local gradients are combined to construct global gradients in each round of aggregation. To preserve gradient information, FedBoosting employs the HE method, *Paillier* [32]. Upon initiation of training, a pair of HE keys are distributed among clients, with the public key being utilized for gradient encryption and the secret key for decryption. After each round of local training, local gradients can be calculated by  $G_r^i = \omega_r^i - \omega_{r-1}$ , where  $\omega_{r-1}$  represents the global weight from the previous round, and  $\omega_r^i$  is the weight after training in the current round.

Encrypting  $G_r^i$  and directly transmitting it to the server is infeasible, as *Paillier* can only process integer values. To circumvent this issue, we propose converting  $G_r^i$  into scaled integer form, denoted as  $G_r^{i'}$ , by multiplying with  $1e^{32}$ . Since the weighting scheme at the server side would violate the integer-only constraint for homomorphic computation, we ensure aggregation correctness by dividing  $G_r^{i'}$  into  $P$  segments and then rounding to an integer according to  $g_r^i = \lfloor G_r^{i'} / P \rfloor$ . This results in negligible precision loss, as only the last few bits are discarded. For instance, with  $P = 10$ , value loss occurs only at the 32-th bit, whereas for  $P = 100$ , the loss occurs at the 31-th and 32-th bits. Finally,  $g_r^i$  is encrypted using *Paillier*, and the encrypted  $g_r^i$  is transmitted to the server. Conversely, the client weight  $p_r$  is converted to an integer by multiplying  $P$  followed by a rounding operation. In FedBoosting, the aggregation weight is computed according to Equ. (2 & 3). The final encrypted global gradients  $G_r^*$  can be computed by merging all gradients from clients (see Equ. (4)). The final encrypted global gradients  $G_r^*$  are then sent back to each client for decryption and global weight generation by  $\omega_r = \omega_{r-1} + G_r^*$ , where  $G_r^*$  is decrypted from  $G_r^*$ . The proposed secure aggregation approach using HE with quantized gradient is generalizable and can also be employed for FedAvg.

$$G_r^* = \sum_i^N \lfloor p_r^i \cdot P \rfloor \cdot g_r^{*i}; \forall p_r^i \in [0, 1] \quad (4)$$

### 3.3 DP Fusion for Local Model Protection

The local gradient between the client and server is safeguarded by HE as previously mentioned. In the proposed FedBoosting mechanism, local models are disseminated to all other clients for cross-validation, and all clients possess an identical key pair. The FedAvg demonstrates that the uniformly amalgamated global model is capable of performing comparably to any local model. Thus, in order to protect gradient privacy among clients, we draw inspiration from DP and suggest perturbing individual local models through a linear combination with HE-encrypted local models, wherein the target model assumes a dominant proportion, yielding the highest weight. Only the perturbed local models are exchanged among clients for cross-validation. Empirically, the reconstructed model exhibits performance akin to that of the local model. Upon receipt of all the encrypted local gradient pieces  $g_r^{*i}, \forall i = 1, 2, \dots, N$  by the server, the server arbitrarily generates  $N$  sets of private fusing weights, within which the corresponding local model consistently assumes the largest proportion. Subsequently, the server computes  $N$  reconstructed local models using HE in accordance with the  $N$  sets of weights (see Equ. 5).

$$\hat{G}_r^{*i} = \lfloor \hat{p} \cdot P \rfloor \cdot g_r^{*i} + \sum_{j:j \neq i}^N \lfloor \frac{(1 - \hat{p}) \cdot P}{N - 1} \rfloor \cdot g_r^{*j} \quad (5)$$

where  $\hat{G}_r^{*i}$  represents the  $i$ -th dual-encrypted whole gradient in round  $r$ . Ultimately, the server disseminates the reconstructed local models to all clients for cross-validation. As DP is employed on the server for linear combination and HE is utilized on the client, the model is rigorously protected during the exchange process between the server and clients. The performance of the local model may decline due to precision loss resulting from the use of quantized HE and linear reconstruction for cross-validation. However, as depicted in Figure 5, our experimental outcomes reveal that there is no substantial loss in testing accuracy. Consequently, the privacy budget  $\epsilon$  can be expressed as the logarithm of the performance drop  $d$  induced by the linear reconstruction, formulated as  $\epsilon = \ln d$ .

## 4 Experiments

### 4.1 Decision Boundary Comparison using Synthetic Dataset

Initially, we performed evaluations employing two datasets to juxtapose the decision boundary between FedAvg and FedBoosting. The task encompasses a binary classification problem with 2D features, facilitating a comprehensible visualization of the decision boundary. We posited that the data adheres to a 2D Gaussian distribution, and two datasets were randomly sampled with distinct mean centers and standard deviations to simulate the Non-IID scenario. Each individual dataset was utilized for train-

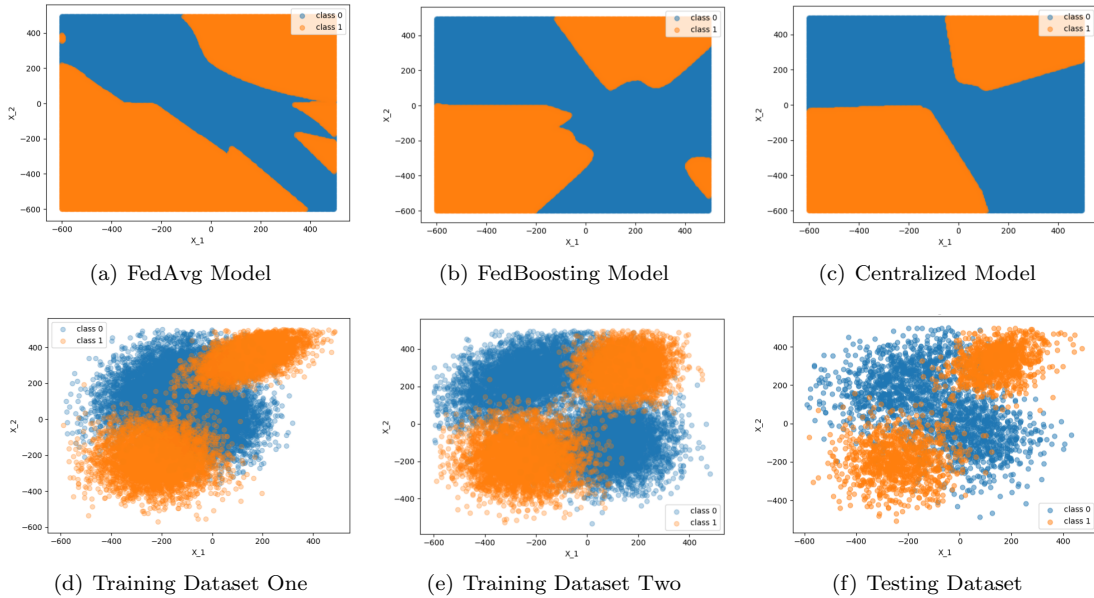


Figure 2: Figures (a), (b), and (c) in the first row illustrate the decision boundaries of global models trained employing FedAvg, FedBoosting, and non-FL methods (centralized training scheme), respectively. Figures (d), (e), and (f) in the second row display two training datasets for two clients within an FL setting and the testing dataset. The model procured in Figure (c) is trained using all datasets, encompassing both (d) and (e).

ing on a client, and the global model was aggregated using FedAvg and the proposed FedBoosting, wherein each dataset contained 40,000 samples and was divided into training and testing sets in a 9:1 ratio. Figure 2 (d), (e), and (f) depict the two training datasets and the combined testing dataset, respectively. A rudimentary neural network was employed, consisting of two fully connected layers followed by a *Sigmoid* activation layer and a *Softmax* layer, respectively. The first fully connected layer contained eight hidden nodes, while the second layer featured two hidden nodes. The *Adam* optimizer with a learning rate of 0.003 was utilized. All models trained via FedBoosting surpassed those trained with FedAvg, employing a batch size of eight and an epoch of one. Figure 2 (a) and (b) display visualizations of the decision boundary of global models trained using FedAvg, FedBoosting, and a centralized training scheme, respectively. It can be inferred that the proposed FedBoosting yields a considerably smoother decision boundary compared to the FedAvg approach. Moreover, the decision boundary of our method more closely resembles the model trained using a centralized scheme, in which both datasets were employed concurrently. This investigation reveals that our method possesses greater generalizability in principle.

## 4.2 Evaluation on Text Recognition Task

We employed Convolutional Recurrent Neural Network (CRNN)[47] as the local neural network model for the text recognition task. CRNN utilizes *VGGNet*[48] as the backbone network for feature extraction, eliminating the fully connected layers and unrolling the feature maps along

the horizontal axis. To model the sequential representation, a multi-layer Bidirectional Long-Short Term Memory (BiLSTM) network [49] is situated atop the convolutional layers, accepting the unrolled visual features as input and modeling the long-term dependencies within the sequence in both directions. The outputs of BiLSTM are channeled into a *Softmax* layer, projecting each element of the unrolled sequence to the probability distribution of potential characters. The character with the highest *Softmax* score is treated as an intermediate prediction. The Connectionist Temporal Classification (CTC) [50] decoder is employed to merge intermediate predictions to generate the final output text. For a comprehensive understanding of the CRNN model, readers are encouraged to consult the original publication [47].

### 4.2.1 Experimental Setting

The proposed model is trained on two extensive synthetic datasets, *Synthetic Text 90k* and *Synthetic Text*, without fine-tuning on other datasets. The model is assessed on four additional standard datasets to evaluate its general recognition performance. For all experiments, word-level accuracy serves as the metric for prediction performance.

**Synthetic Text 90k** [51] (Synth90K) constitutes one of two training datasets employed in this paper. This dataset comprises approximately 7.2 million images and their corresponding ground truth words. For FedBoosting, we divide the images into two subsets: the first containing 6.5 million images for training, and the second consisting of 0.7 million images for validation.

**Synthetic Text** [51] (SynthText) serves as the sec-

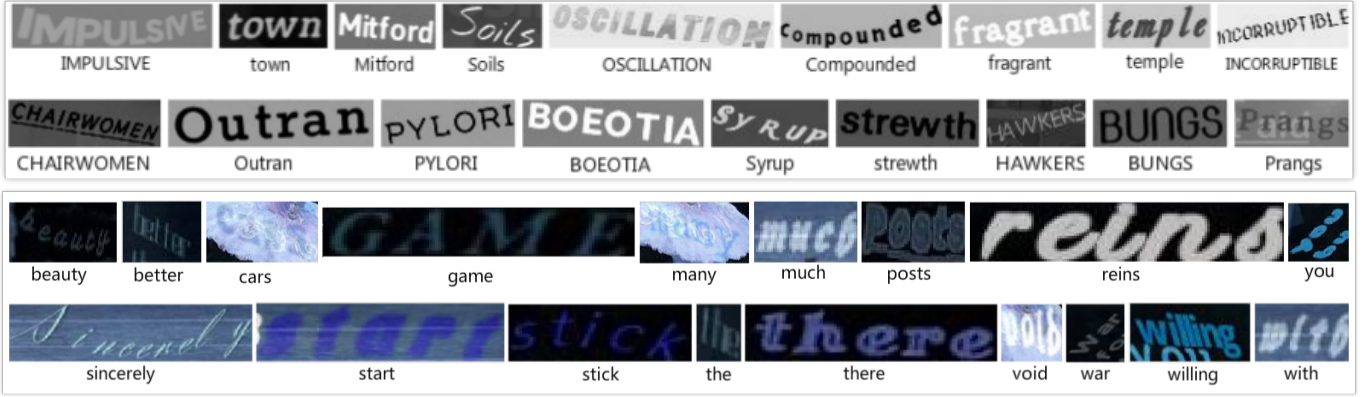


Figure 3: The visual example of training images is derived from the *Synth90K* (top two rows) and *SynthText* (bottom two rows) datasets.

Table 1: Recognition accuracies (%) are presented for four testing datasets. The abbreviations “90K” and “ST” represent the *Synth90K* and *SynthText* datasets, respectively. The results in the first row (CRNN\*) and the second row (CRNN) are obtained from the standard CRNN model without employing the FL framework. Here, CRNN\* corresponds to accuracies reported in [47], while CRNN denotes the results reproduced using our implementation.

Method	Dataset	#Batch	#Epoch	IIIT5K	SVT	SCUT	IC15
CRNN*	90K	-	-	81.20	82.70	-	-
CRNN	ST	512	-	76.07	77.60	89.38	55.92
	ST	800	-	73.69	78.00	86.94	58.88
	90K	512	-	80.95	86.40	87.49	67.43
	90K	800	-	80.71	83.60	87.80	62.50
	ST & 90K	512	-	83.81	90.40	93.08	71.71
	ST & 90K	800	-	85.48	88.00	93.78	72.70
FedAvg	ST & 90K	256	1	-	-	-	-
	ST & 90K	256	3	-	-	-	-
	ST & 90K	512	1	85.48	87.60	93.31	73.36
	ST & 90K	512	3	80.83	87.60	91.11	64.80
	ST & 90K	800	1	86.67	89.60	94.49	72.37
	ST & 90K	800	3	81.82	88.00	93.47	70.07
Ours	ST & 90K	256	1	85.83	89.2	94.26	72.37
	ST & 90K	256	3	84.88	91.20	<b>94.65</b>	70.07
	ST & 90K	512	1	85.12	88.00	93.39	74.34
	ST & 90K	512	3	87.38	90.80	93.86	70.39
	ST & 90K	800	1	<b>87.62</b>	89.20	94.18	<b>75.99</b>
	ST & 90K	800	3	85.60	<b>91.60</b>	<b>94.65</b>	70.72

ond training dataset utilized. This dataset contains approximately 85K natural images featuring numerous synthetic texts. We crop all texts using labeled text bounding boxes to create a new dataset of 5.3 million text images. For FedBoosting, we partition this dataset into a training dataset of 4.8 million images and a validation dataset of 0.5 million images.

**IIIT 5K-Words** [52] (IIIT5K) is sourced from the internet and encompasses 3000 cropped word images in its testing set, with each image containing a ground truth word.

**Street View Text** [53] (SVT) is derived from *Google Street View* and consists of 647 word images in its testing set. Many images in this dataset are significantly degraded by noise and blur or exhibit extremely low resolutions.

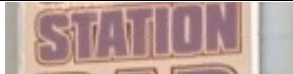









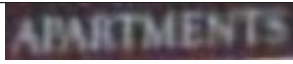




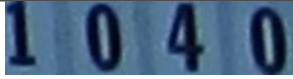

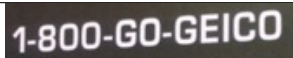
**SCUT-FORU** [54] (SCUT) includes 813 training images and 349 testing images, characterized by significant variations in background and illumination.

**ICDAR 2015** [55] (IC15) comprises 2077 cropped images that feature relatively low resolutions and multi-oriented texts. For a fair comparison, we exclude images containing non-alphanumeric characters, resulting in a final count of 1811 images.

Figure 3 presents visual instances from the *Synth90K* and *SynthText* datasets, illustrating considerable variations in backgrounds and texts between the two sets. Consequently, it can be deduced that these datasets exhibit Non-IID characteristics. To accommodate mini-batch processing and expedite the training procedure, all training and validation images are resized to dimensions of  $100 \times 32$ .



Table 2: A visual representation of testing outcomes is provided, utilizing FedAvg and FedBoosting models with a batch size of 512 and an epoch count of 3. Erroneously predicted characters are emphasized in red, and green characters enclosed in brackets signify those omitted from the predictions.

Samples	FedAvg	FedBoosting
	MOUNT <b>R</b> IN	MOUNTAIN
	STATION <b>NN</b>	STATION
	MANHAT <b>I</b> TAN	MANHATTAN
	PL <b>A</b> ZZA	PIAZZA
	VIRG <b>(I)</b> N	VIRGIN
	MAXI <b>V</b> US	MAXIMUS
	<b>U</b> GREEN <b>N</b>	GREEN
	<b>J</b> ECOIL	ECOIL
	DIR <b>(E)</b> CI <b>N</b>	DIRECTORY
	CEN <b>R</b> AL	CENTRAL
	CAN <b>S</b> Y	CANDY
	<b>A</b> BARTMENTS	APARTMENTS
	WORKSHOP <b>(E)</b>	WORKSHOPE
	T <b>I</b> SC	TSC
	CRI <b>A</b> VEN	CRAVEN
	<b>20</b> MBIES	ZOMBIES
	<b>3</b> 44	844
	<b>17</b> 040	1040
	100 <b>1</b> 000	100000
	1800GO <b>G</b> GEI <b>C</b> O	1800G <b>O</b> GEI <b>C</b> O

In Tables 1 and 3, testing images are proportionally resized to maintain a height of 32 pixels. Figures 4, 5,

and 6 display testing images processed identically to the aforementioned training and validation images. Due to



the constraints imposed by CTC, testing images with label lengths less than 3 or greater than 25 characters are excluded. The *Synth90K* and *SynthText* datasets are deployed on two distinct clients, with *AdaDelta* employed for back-propagation optimization on local training nodes, and an initial learning rate of 0.05. For HE, a key size of 128 bits is utilized, and the entire gradient is divided into 100 segments with  $\hat{p} = 0.9$ . Our method is implemented using *Keras* and *Tensorflow* in a distributed multi-GPUs setup, with the source code publicly accessible to ensure reproducibility.

#### 4.2.2 Result and Discussion

Table 1 presents a comparative analysis of test dataset outcomes using various training hyperparameters, including batch size and number of epochs. The first row (CRNN\*) and the second row (CRNN) represent results produced by the original CRNN model without employing the FL framework, where CRNN\* corresponds to the accuracies reported by its authors in [47], and CRNN corresponds to the results we reproduced. In comparison to the original CRNN model, FedAvg exhibits a substantial improvement. For instance, the FedAvg model with a batch size of 800 and an epoch of 1 achieves an accuracy of 86.67% on the *IIIT5k* dataset, signifying a 1.19% enhancement compared to the CRNN result of 85.48% using the same configuration. The FedAvg model with a batch size of 512 and an epoch of 1 exhibits a 1.65% improvement on the *IC15* dataset. More significantly, the proposed FedBoosting method attains the highest accuracy across all four test datasets, with 87.62%, 91.60%, 94.65%, and 75.99% reported on *IIIT5k*, *SVT*, *SCUT*, and *IC15*, respectively. Additionally, our approach outperforms both FedAvg and non-FL methods by considerable margins. Table 2 provides more qualitative results.

It can be observed that FedAvg models with larger batch sizes and fewer epochs exhibit superior performance. In other words, the models perform better when model integration occurs more frequently, albeit at the expense of increased communication costs. In Table 1, the model with a batch size of 256 and one epoch does not produce a result due to model divergence after several integration rounds. The potential reason could be the extreme differences in parameters learned on each local machine. Figure 4 compares the convergence curves of FedAvg and the proposed FedBoosting. The convergence curves of FedAvg models with smaller batch sizes or more epochs are consistently lower than those of models with larger batch sizes or fewer epochs. For instance, employing the FedAvg strategy, the model with a batch size of 800 and one epoch (iterating 6,689 and 9,030 times per epoch on the *SynthText* and *Synth90K* datasets, respectively) performs significantly better than the model with a batch size of 512 and three epochs (iterating 10,452 and 14,110 times per epoch on the *SynthText* and *Synth90K* datasets, respectively) on the *IIIT5K* test dataset. Conversely, the accuracy curves of FedBoosting models (as seen in Figure 4, second row) do

not exhibit this issue. Consequently, we deduce that the proposed boosting strategy effectively mitigates the model collapse issue of FedAvg to a significant extent.

Table 3: Recognition accuracies (%) on three testing datasets. All experiments are using batch size of 800 and epoch of 1.

Method	Encryption	IIIT5K	SVT	IC15
FedAvg	N/A	86.67	<b>89.60</b>	72.37
	HE	86.40	88.00	73.00
FedBoosting	N/A	<b>87.62</b>	89.20	<b>75.99</b>
	HE	85.12	88.40	72.70
	HE+DP	85.00	88.80	72.37

Table 4: Validation accuracies from local models without and with linear reconstruction.

Client	#Batch/#Epoch	w/o DP	w/ DP	Gap
1	256/1	94.34%	92.23%	-2.11%
2		90.32%	86.83%	-3.49%
1	256/3	95.81%	92.82%	-2.99%
2		90.26%	86.92%	-3.34%
1	512/1	94.09%	92.31%	-1.78%
2		88.34%	85.29%	-3.05%
1	512/3	96.46%	92.89%	-3.57%
2		91.84%	86.71%	-5.13%
1	800/1	94.71%	92.52%	-2.19%
2		89.44%	87.19%	-2.25%
1	800/3	97.08%	92.74%	-4.34%
2		93.45%	87.91%	-5.54%

Table 3 presents a comparative analysis of three testing datasets (*IIIT5K*, *SVT*, and *IC15*) using various FL gradient merging techniques and encryption modes, given hyperparameters of 800 batch size and 1 epoch. The results for FedAvg indicate that, although employing HE results in a minor precision loss due to the partitioning of the entire gradient into multiple pieces, accuracy is virtually unaffected on the testing datasets. In fact, there is an increase in accuracy on the *IC15* dataset from 72.37% to 73.00%. On the remaining two testing datasets, the accuracy losses are 0.27% and 1.6%, respectively. Similarly, for FedBoosting models, testing outcomes exhibit a slight accuracy reduction, which can be tolerated when using HE exclusively. When incorporating DP with HE in FedBoosting, the accuracy of the global model remains largely unaffected. This is because DP encryption is only employed to encrypt local gradients between clients for evaluation and to obtain results on all clients' validation datasets. Table 4 illustrates the impact of DP on local model performance. Validation experiments using DP are conducted on individual clients, necessitating the incorporation of HE. We hypothesize that HE has a minimal effect on validation accuracy since it only modifies the final two digits out of 32 decimal places. The disturbance to  $p_r$  is

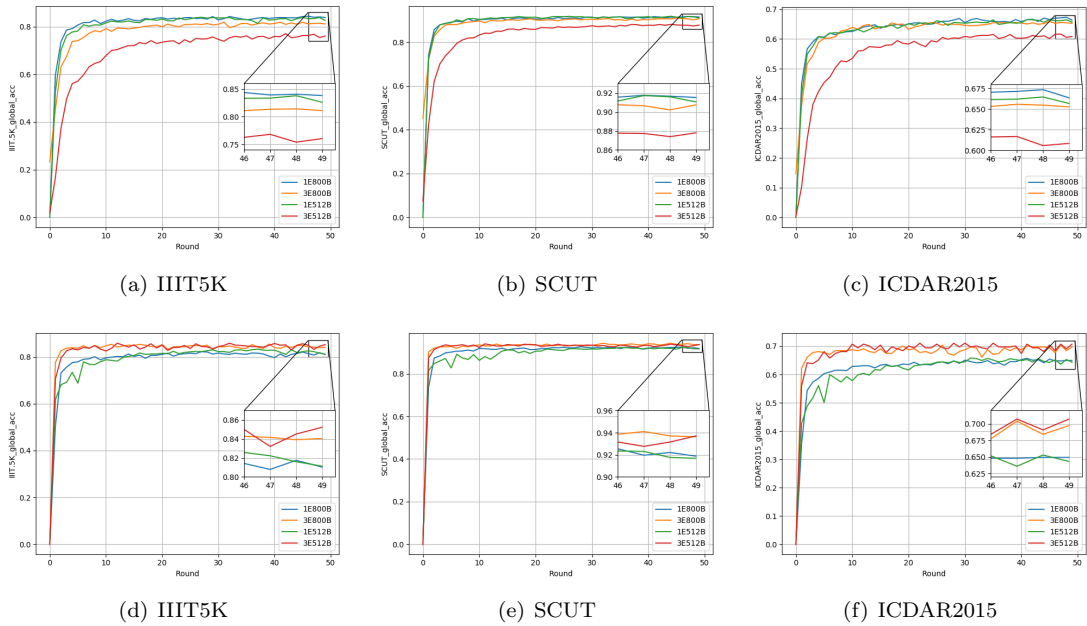


Figure 4: Testing accuracies of FedAvg (first row) and FedBoosting (second row) models across rounds for the *IIIT5K*, *SCUT*, and *IC15* datasets are presented. The notation "1E800B" denotes that the model is trained on a client with a batch size of 800 and one epoch. All samples in these testing subsets are resized to  $100 \times 32$ , differing from the processing in Table 1.

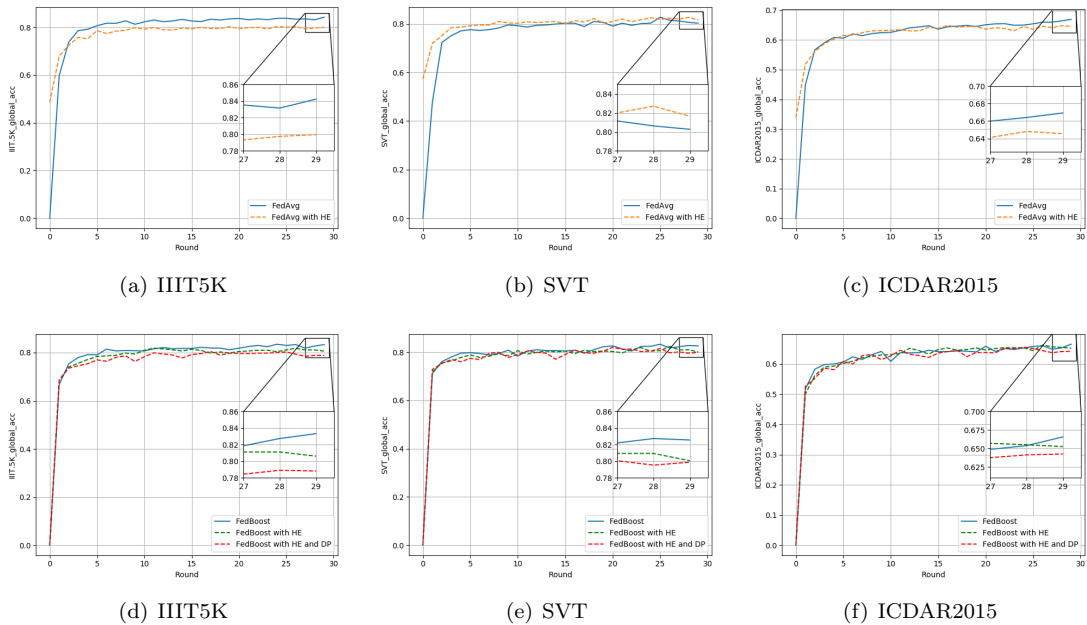
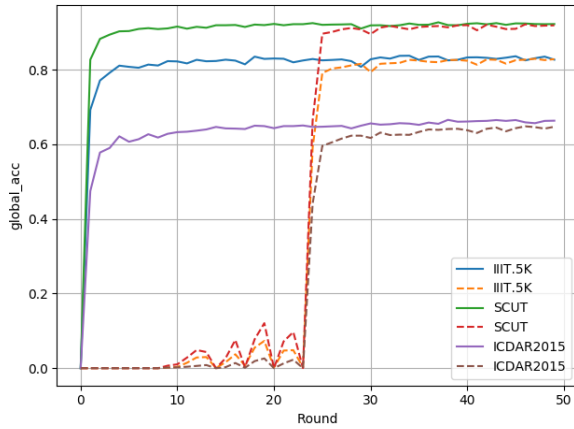


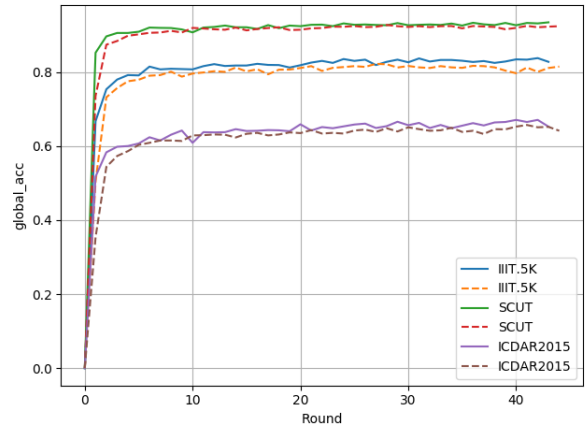
Figure 5: Testing accuracy of FedAvg (first row) and FedBoosting (second row) models with and without using encryption protocol over training rounds on *IIIT5K*, *SVT* and *IC15* datasets.

relatively insignificant, as referred to in Equation 2, leading to the conclusion that DP has limited influence on the generation of global gradients. Nevertheless, testing results exhibit a decline between standard FedBoosting and encrypted FedBoosting models, for example, accuracy is reduced from 87.62% to approximately 85.00% on *IIIT5K* and around 3.00% on *IC15*. This is a typical fluctuation

for training DL models. Although testing accuracies for all three datasets exhibit varying degrees of reduction, the accuracy growth trends are represented by the differential curves under different encryption modes in Figure 5. It can be observed that the differentials for most testing datasets are relatively small.



(a) 256 batch size and 1 epoch



(b) 800 batch size and 1 epoch

Figure 6: Performance comparison on how the training results affect the model performance. Solid lines refer to global models aggregated with training and validation results, while dash lines refer to global models aggregated only with validation results.

### 4.2.3 Performance Comparison

We further posit that the divergence issue can be attributed to the quality of the datasets, as illustrated in Figure 3. In other words, each local model trained on distinct private datasets undoubtedly possesses varying generalization capabilities. In our experiments, the crude aggregation of the global model by averaging the weights of local models may lead to a decline in generalization ability, particularly when the number of local updating iterations is large (i.e., small batch size or large epoch number). Consequently, the proposed FedBoosting aims to assign a more equitable weight instead of a mean value by balancing the training and validation performance of a local model. Guided by this rationale, FedBoosting initially takes into account each model’s validation results on every client’s validation dataset and subsequently incorporates training results to compute the weights of local models. The consideration of training results stems from the fact that a local model trained on a high-quality dataset typically exhibits a satisfactory fitness, which may, however, perform poorly on low-quality validation datasets. It would be unjust to deem this model as having inadequate generalization ability based solely on its validation performance across datasets of varying quality. Conversely, a model trained on a poor-quality dataset might excel on a high-quality validation dataset; however, we do not desire this type of local model to dominate the global model. As a result, to balance the performance of a local model, we initially aggregate the validation results as a reference representing the local model’s generalization ability. Moreover, training results are factored in to adjust the reference and derive the final weights for each local model. Our experiments reveal that the weights amount to approximately 55.00% for the local model trained on the *Synth90K* dataset and 45.00% on the *SynthText* dataset, which is reasonable con-

sidering the accuracy results in Table 1 that CRNN models trained on the *Synth90K* dataset consistently outperform those trained on the *SynthText* dataset. If we disregard training results, the weight for the local model trained on the *Synth90K* dataset would be smaller than that on the *SynthText* dataset.

To prove the above idea in FedBoosting, a performance comparison is given here. It is commonly accepted that generalization ability is a good metrics of judging a model’s performance, whereas only considering generalization ability is not feasible for our proposed method FedBoosting. Otherwise, it is impossible as well to deploy our method only considering training results and get rid of validation results, which may lead to an extremely unfair situation that local model trained on *Synth90K* may take a weight up to about 80% for the global model. So the following content is mainly talking about how training results work in FedBoosting. We trained a global model with 256 batch size and 1 epoch under the strategy of FedBoosting without considering training results. As described above, the reason of thinking over training results is to rectify the weight for local model. From Figure 6 (a), we can see that the global model without taking training results gains a delay convergence at round 24. While in other experiments, models all converge quickly and properly under the supervision of training results. In the meantime, the performance of global model with training results is always better than that without training results. As a supplement, we visualize the global testing accuracy of two models with 800 batch size and 1 epoch in Figure 6 (b), one uses training results and the other one does not. Two models converge normally in this case, but the model performance of using training results outperforms all the time. From all above, we consider that using training results to supervise the local weight is essential in our scenario. To clarify,

all testing images during training are resized to  $100 \times 32$ , which is different to individual testing experiments where testing images are resized to  $W \times 32$ , where  $W$  is the proportionally scaled with heights, but at least 100 pixels. That is why accuracies in Figure 6 are lower than those in Table 1. Please refer to our codes for more details.

In order to substantiate the aforementioned concept within the FedBoosting framework, a comparative analysis of performance is presented herein. It is widely acknowledged that a model’s generalization ability serves as a reliable metric for evaluating performance; however, relying solely on generalization ability is not tenable for our proposed FedBoosting methodology. Likewise, implementing our approach by solely taking into account training outcomes while disregarding validation results may lead to an egregiously unjust scenario in which a local model trained on *Synth90K* might contribute up to approximately 80.00% of the weight for the global model. Consequently, the subsequent discussion primarily focuses on the role of training outcomes in FedBoosting. We trained a global model employing a 256 batch size and a single epoch under the FedBoosting strategy, without considering training results. The impetus for incorporating training outcomes is to adjust the local model’s weight. As depicted in Figure 6 (a), a global model that excludes training results exhibits delayed convergence at round 24. Conversely, in other experiments, models consistently exhibit rapid and appropriate convergence under the guidance of training results. Simultaneously, the performance of the global model that incorporates training results consistently surpasses that of the model which does not. Additionally, we provide a visualization of the global testing accuracy for two models with an 800 batch size and a single epoch in Figure 6 (b); one model employs training results while the other does not. Both models demonstrate normal convergence in this instance, but the performance of the model utilizing training results consistently excels. Based on the aforementioned evidence, we posit that supervising local weight with training results is indispensable in our context. For clarity, all testing images during training are resized to  $100 \times 32$ , which differs from individual testing experiments where testing images are resized to  $W \times 32$ , where  $W$  is proportionally scaled with heights but maintains a minimum of 100 pixels. This discrepancy accounts for the lower accuracies observed in Figure 6 compared to those in Table 1. Further details can be found in our code documentation.

## 5 Conclusion

In the present study, we introduced FedBoosting, a boosting scheme for the FL framework, to address the limitations of the FedAvg algorithm on Non-IID datasets. To safeguard against gradient leakage attacks, a gradient-sharing protocol incorporating HE and DP was devised. A thorough comparative analysis was conducted using synthetic datasets and public text recognition benchmarks,

demonstrating superior performance compared to traditional FedAvg schemes on Non-IID datasets. Our implementation is publicly accessible to ensure reproducibility and is compatible with distributed multi-GPUs setups. Potential areas for future exploration include the theoretical examination of model convergence within multi-party computing, privacy leakage risks associated with gradients, and the development of more efficient gradient quantization methods.

## Acknowledgment

This work was supported by the Engineering and Physical Sciences Research Council (EPSRC) UK, Data Release - Trust, Identity, Privacy and Security [Grant Number: EP/N028139/1].

## References

- [1] Y. Aono, T. Hayashi, L. Wang, S. Moriai, *et al.*, “Privacy-preserving deep learning via additively homomorphic encryption,” *IEEE TIFS*, vol. 13, no. 5, pp. 1333–1345, 2017.
- [2] E. Hesamifard, H. Takabi, M. Ghasemi, and R. N. Wright, “Privacy-preserving machine learning as a service,” *Proceedings on Privacy Enhancing Technologies*, vol. 2018, no. 3, pp. 123–142, 2018.
- [3] T. Ryffel, A. Trask, M. Dahl, B. Wagner, J. Mancuso, D. Rueckert, and J. Passerat-Palmbach, “A generic framework for privacy preserving deep learning,” *arXiv preprint arXiv:1811.04017*, 2018.
- [4] M. Al-Rubaie and J. M. Chang, “Privacy-preserving machine learning: Threats and solutions,” *IEEE S&P*, vol. 17, no. 2, pp. 49–58, 2019.
- [5] J. Liu and X. Meng, “Survey on privacy-preserving machine learning,” *JCRD*, vol. 57, no. 2, p. 346, 2020.
- [6] H. C. Tanuwidjaja, R. Choi, S. Baek, and K. Kim, “Privacy-preserving deep learning on machine learning as a service—a comprehensive survey,” *IEEE Access*, vol. 8, pp. 167425–167447, 2020.
- [7] N. Koti, M. Pancholi, A. Patra, and A. Suresh, “{SWIFT}: Super-fast and robust privacy-preserving machine learning,” in *Security Symposium*, 2021.
- [8] J. Konečný, H. B. McMahan, F. X. Yu, P. Richtárik, A. T. Suresh, and D. Bacon, “Federated learning: Strategies for improving communication efficiency,” *arXiv preprint arXiv:1610.05492*, 2016.
- [9] B. McMahan, E. Moore, D. Ramage, S. Hampson, and B. A. y Arcas, “Communication-efficient learning of deep networks from decentralized data,” in *AIS*, pp. 1273–1282, PMLR, 2017.

- [10] P. Kairouz, H. B. McMahan, B. Avent, A. Bellet, M. Bennis, A. N. Bhagoji, K. Bonawitz, Z. Charles, G. Cormode, R. Cummings, *et al.*, “Advances and open problems in federated learning,” *arXiv preprint arXiv:1912.04977*, 2019.
- [11] J. Konečný, H. B. McMahan, F. X. Yu, P. Richtárik, A. T. Suresh, and D. Bacon, “Federated learning: Strategies for improving communication efficiency,” *arXiv preprint arXiv:1610.05492*, 2016.
- [12] T. Li, A. K. Sahu, M. Zaheer, M. Sanjabi, A. Talwalkar, and V. Smith, “Federated optimization in heterogeneous networks,” *arXiv preprint arXiv:1812.06127*, 2018.
- [13] V. Smith, C.-K. Chiang, M. Sanjabi, and A. S. Talwalkar, “Federated multi-task learning,” in *NIPS*, pp. 4424–4434, 2017.
- [14] Y. Zhao, M. Li, L. Lai, N. Suda, D. Civin, and V. Chandra, “Federated learning with non-iid data,” *arXiv preprint arXiv:1806.00582*, 2018.
- [15] M. G. Arivazhagan, V. Aggarwal, A. K. Singh, and S. Choudhary, “Federated learning with personalization layers,” *arXiv preprint arXiv:1912.00818*, 2019.
- [16] P. P. Liang, T. Liu, L. Ziyin, N. B. Allen, R. P. Auerbach, D. Brent, R. Salakhutdinov, and L.-P. Morency, “Think locally, act globally: Federated learning with local and global representations,” *arXiv preprint arXiv:2001.01523*, 2020.
- [17] T. Lin, L. Kong, S. U. Stich, and M. Jaggi, “Ensemble distillation for robust model fusion in federated learning,” *NIPS*, vol. 33, pp. 2351–2363, 2020.
- [18] C. Li, G. Li, and P. K. Varshney, “Decentralized federated learning via mutual knowledge transfer,” *IEEE IoT*, vol. 9, no. 2, pp. 1136–1147, 2021.
- [19] D. Li and J. Wang, “Fedmd: Heterogenous federated learning via model distillation,” *arXiv preprint arXiv:1910.03581*, 2019.
- [20] X. Peng, Z. Huang, Y. Zhu, and K. Saenko, “Federated adversarial domain adaptation,” *arXiv preprint arXiv:1911.02054*, 2019.
- [21] A. Ghosh, J. Chung, D. Yin, and K. Ramchandran, “An efficient framework for clustered federated learning,” *NIPS*, vol. 33, pp. 19586–19597, 2020.
- [22] C. Briggs, Z. Fan, and P. Andras, “Federated learning with hierarchical clustering of local updates to improve training on non-iid data,” in *IJCNN*, pp. 1–9, IEEE, 2020.
- [23] X. Li, K. Huang, W. Yang, S. Wang, and Z. Zhang, “On the convergence of fedavg on non-iid data,” *arXiv preprint arXiv:1907.02189*, 2019.
- [24] Y. Chen, X. Yang, X. Qin, H. Yu, P. Chan, and Z. Shen, “Dealing with label quality disparity in federated learning,” *Federated Learning: Privacy and Incentive*, pp. 108–121, 2020.
- [25] B. Pejó, A. Tóth, and G. Biczók, “Quality inference in federated learning with secure aggregation,” *arXiv preprint arXiv:2007.06236*, 2020.
- [26] M. Fredrikson, S. Jha, and T. Ristenpart, “Model inversion attacks that exploit confidence information and basic countermeasures,” in *ACM SIGSAC CCCS*, pp. 1322–1333, 2015.
- [27] L. Melis, C. Song, E. De Cristofaro, and V. Shmatikov, “Exploiting unintended feature leakage in collaborative learning,” in *IEEE S&P*, pp. 691–706, IEEE, 2019.
- [28] B. Hitaj, G. Ateniese, and F. Perez-Cruz, “Deep models under the gan: information leakage from collaborative deep learning,” in *ACM SIGSAC CCCS*, pp. 603–618, 2017.
- [29] L. Zhu, Z. Liu, and S. Han, “Deep leakage from gradients,” in *NIPS*, pp. 14774–14784, 2019.
- [30] B. Zhao, K. R. Mopuri, and H. Bilen, “idlg: Improved deep leakage from gradients,” *arXiv preprint arXiv:2001.02610*, 2020.
- [31] H. Ren, J. Deng, and X. Xie, “Grnn: Generative regression neural network—a data leakage attack for federated learning,” *ACM TIST*, 2021.
- [32] P. Paillier, “Public-key cryptosystems based on composite degree residuosity classes,” in *ICTACT*, pp. 223–238, Springer, 1999.
- [33] B. McMahan and D. Ramage, “Federated learning: Collaborative machine learning without centralized training data,” *Google Research Blog*, vol. 3, 2017.
- [34] Q. Yang, Y. Liu, Y. Cheng, Y. Kang, T. Chen, and H. Yu, “Federated learning,” *SLAIML*, vol. 13, no. 3, pp. 1–207, 2019.
- [35] W. Zhang, Y. Qiu, S. Bai, R. Zhang, X. Wei, and X. Bai, “Fedocr: Communication-efficient federated learning for scene text recognition,” *arXiv preprint arXiv:2007.11462*, 2020.
- [36] A. C.-C. Yao, “How to generate and exchange secrets,” in *SFCS*, pp. 162–167, IEEE, 1986.
- [37] O. Goldreich, “Secure multi-party computation,” *Manuscript. Preliminary version*, vol. 78, 1998.
- [38] M. Hao, H. Li, G. Xu, S. Liu, and H. Yang, “Towards efficient and privacy-preserving federated deep learning,” in *ICC*, pp. 1–6, IEEE, 2019.

- [39] C. Xu, J. Ren, D. Zhang, Y. Zhang, Z. Qin, and K. Ren, “Ganobfuscator: Mitigating information leakage under gan via differential privacy,” *IEEE TIFS*, vol. 14, no. 9, pp. 2358–2371, 2019.
- [40] J. Zhao, Y. Chen, and W. Zhang, “Differential privacy preservation in deep learning: Challenges, opportunities and solutions,” *IEEE Access*, vol. 7, pp. 48901–48911, 2019.
- [41] D. Byrd and A. Polychroniadou, “Differentially private secure multi-party computation for federated learning in financial applications,” *arXiv preprint arXiv:2010.05867*, 2020.
- [42] S. Truex, N. Baracaldo, A. Anwar, T. Steinke, H. Ludwig, R. Zhang, and Y. Zhou, “A hybrid approach to privacy-preserving federated learning,” in *ACM AIS*, pp. 1–11, 2019.
- [43] S. Hardy, W. Henecka, H. Ivey-Law, R. Nock, G. Patrini, G. Smith, and B. Thorne, “Private federated learning on vertically partitioned data via entity resolution and additively homomorphic encryption,” *arXiv preprint arXiv:1711.10677*, 2017.
- [44] C. Zhang, S. Li, J. Xia, W. Wang, F. Yan, and Y. Liu, “Batchcrypt: Efficient homomorphic encryption for cross-silo federated learning,” in *2020 Annual Technical Conference*, pp. 493–506, 2020.
- [45] H. Fang and Q. Qian, “Privacy preserving machine learning with homomorphic encryption and federated learning,” *FI*, vol. 13, no. 4, p. 94, 2021.
- [46] C. Xu, Z. Hong, M. Huang, and T. Jiang, “Acceleration of federated learning with alleviated forgetting in local training,” *arXiv preprint arXiv:2203.02645*, 2022.
- [47] B. Shi, X. Bai, and C. Yao, “An end-to-end trainable neural network for image-based sequence recognition and its application to scene text recognition,” *IEEE TPAMI*, vol. 39, no. 11, pp. 2298–2304, 2016.
- [48] K. Simonyan and A. Zisserman, “Very deep convolutional networks for large-scale image recognition,” *arXiv preprint arXiv:1409.1556*, 2014.
- [49] A. Graves, M. Liwicki, S. Fernández, R. Bertolami, H. Bunke, and J. Schmidhuber, “A novel connectionist system for unconstrained handwriting recognition,” *IEEE TPAMI*, vol. 31, no. 5, pp. 855–868, 2008.
- [50] A. Graves, S. Fernández, F. Gomez, and J. Schmidhuber, “Connectionist temporal classification: labelling unsegmented sequence data with recurrent neural networks,” in *ICML*, pp. 369–376, ACM, 2006.
- [51] M. Jaderberg, K. Simonyan, A. Vedaldi, and A. Zisserman, “Synthetic data and artificial neural networks for natural scene text recognition,” *arXiv preprint arXiv:1406.2227*, 2014.
- [52] A. Mishra, K. Alahari, and C. Jawahar, “Scene text recognition using higher order language priors,” 2012.
- [53] K. Wang, B. Babenko, and S. Belongie, “End-to-end scene text recognition,” in *ICCV*, pp. 1457–1464, IEEE, 2011.
- [54] S. Zhang, M. Lin, T. Chen, L. Jin, and L. Lin, “Character proposal network for robust text extraction,” in *ICASSP*, pp. 2633–2637, IEEE, 2016.
- [55] D. Karatzas, L. Gomez-Bigorda, A. Nicolaou, S. Ghosh, A. Bagdanov, M. Iwamura, J. Matas, L. Neumann, V. R. Chandrasekhar, S. Lu, *et al.*, “Icdar 2015 competition on robust reading,” in *ICDAR*, pp. 1156–1160, IEEE, 2015.